Partial encapsulation of Pd particles by reduced ceria-zirconia

H. P. Sun and X. P. Pan[a)]
Department of Materials Science and Engineering, University of Michigan, Ann Arbor, Michigan 48109-2136

G. W. Graham, H.-W. Jen, and R. W. McCabe
Chemical Engineering Department, Ford Research Laboratory, Dearborn, Michigan 48121

S. Thevuthasan and C. H. F. Peden
Pacific Northwest National Laboratory, P.O. Box 999, Richland, Washington 99352

(Received 17 February 2005; accepted 22 September 2005; published online 11 November 2005)

Direct observation of metal-oxide interfaces with atomic resolution can be achieved by cross-sectional high-resolution transmission electron microscopy (HRTEM). Using this approach to study the response of a model, single-crystal thin film automotive exhaust-gas catalyst, Pd particles supported on the (111) ceria-zirconia (CZO) surface, to a redox cycle, we have found two distinct processes for the partial encapsulation of the Pd particles by the reduced CZO surface that depend on their relative crystallographic orientations. In the case of the preferred orientation found for Pd particles on CZO, Pd(111)[110]//CZO(111)[110], a flat and sharp metal/oxide interface was maintained upon reduction, while ceria-zirconia from the adjacent surface tended to accumulate on and around the Pd particle. In rare cases, Pd particles with other orientations tended to sink into the oxide support upon reduction. Possible mechanisms for these encapsulation processes are proposed. © *2005 American Institute of Physics*. [DOI: 10.1063/1.2132067]

The interaction between metal particles and their oxide support attracts much research interest.[1–3] The concept of strong metal-support interaction (SMSI)[4] is often used to describe the effect of the support on the catalytic activity of the metal. Generally, facile reducibility of the oxide is a prerequisite for the observation of SMSI-like effects, and TiO_2, as one such oxide, has often been used in the study of SMSI. The interaction of Pd nanoparticles with TiO_2, for example, was studied by high temperature scanning tunneling microscopy (STM).[5] Additionally, Bernal and co-workers[6–8] have done a considerable amount of high-resolution transmission electron microscopy (HRTEM) work on ceria-supported precious-metal catalysts (mostly the Pt and Rh systems) using powder samples. Ceria is an important ingredient in the modern automotive three-way catalyst (TWC),[9] which is a complex mixture of precious-metal particles (Pt, Rh, Pd) and various oxide materials. The addition of ceria (CeO_2) to the support greatly enhances TWC performance, in part because of the ability of ceria to store and release oxygen. Recently, ceria has been replaced by ceria-zirconia mixed oxide, which provides even better oxygen storage and release properties as well as improved thermal stability.[10,11] For the TWC, operating at high temperature under cycled redox conditions over long times, potentially damaging interactions between the metal and oxide components cannot be avoided. For example, a substantial fraction of Pd can become encapsulated by the ceria-zirconia mixed oxide under certain conditions.[12–16] Partial encapsulation of metal particles by their oxide support was found many years ago, in the Pt/SiO_2 system.[17] However, surface characterization methods such as scanning electron microscopy (SEM) and STM cannot give a cross-sectional view of encapsulated particles, which is needed to reveal interfacial atomic structure. Such information that is critical for understanding the mechanism of SMSI can be obtained by HRTEM, but control over sample geometry is limited in the case of powder samples. In this work, we have thus performed a cross-sectional HRTEM study of a well-defined thin-film model catalyst: Pd particles on a ceria-zirconia single-crystal surface. The response of the microstructure of the supported Pd particles to a reduction and oxidation (redox) cycle was studied in order to obtain further detailed insight into the encapsulation phenomenon.

A 50 nm thick $Ce_{0.7}Zr_{0.3}O_2$ (ceria-zirconia or CZO) thin film was first grown on the (111) plane of an yttria-stabilized zirconia, ZrO_2:Y (YSZ), substrate by oxygen-plasma-assisted molecular beam epitaxy (MBE).[18] Then, a monolayer-equivalent of Pd was deposited at room temperature onto the CZO thin film in ultra high vacuum (UHV). After calcination (heating in air) at 600 °C for 1 h, the sample was cut into four pieces. One of them (calcined sample) was used to characterize the initial state. A second one (reduced sample) was reduced in a $1\%(H_2+CO)/N_2$ environment at 200 °C for 10 min and then heated to 700 °C, held for 1 h, and cooled to 50 °C, all under N_2. The third one (re-oxidized sample) was reduced in the same manner as the previous sample and then re-oxidized in a $0.5\%O_2/N_2$ environment at 700 °C for 1 hour and cooled to 50 C under N_2. The last piece (extended reduced sample) was twice subjected to the same procedure as the previous reduced sample, except that the heat treatment at 700 °C lasted for 5 h. (The conditions selected were similar to those used for testing the activity of model powder catalyst samples.) Cross-sectional TEM specimens of all the samples were prepared by following the normal procedure including mechanical polishing and Ar+ ion milling. A JEOL-2010F field emission gun TEM equipped with an x-ray energy dispersive spectrometer (EDS) and a Gatan Image Filter (GIF) was used to examine the samples.

TEM images of the calcined sample, e.g., Fig. 1(a), show that the typical Pd particle size at this stage is about 5 nm. After reduction, the Pd particle is in a metallic state. Its

a)Author to whom correspondence should be addressed; electronic mail: panx@umich.edu

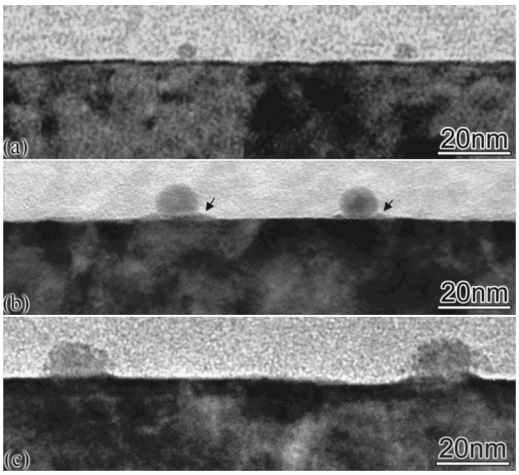

FIG. 1. Cross-sectional TEM images of the Pd particles on the CZO surface after (a) calcination, (b) reduction, and (c) re-oxidation.

shape is similar to that of a projection view of a truncated octahedron with a more-or-less rounded top surface and a flat, sharp interface with the oxide support, as shown in Fig. 1(b). The most frequently observed orientation has Pd(111)//CZO(111). The average particle size is about 10 nm. A prominent morphological characteristic of the reduced sample is that the ceria-zirconia support tends to cover the lower part of such Pd particles. As indicated by arrows in Figs. 1(b), material from the CZO film is present around the Pd particles above the level of the metal-oxide interface. After the re-oxidation treatment, the Pd particle is oxidized into polycrystalline PdO with an average particle size of about 20 nm, as shown in Fig. 1(c). Occasionally, we found a Pd particle that appeared to have sunk into the support after reduction, resulting in a curved interface, as shown in Fig. 2. In this case, the Pd particle shows a different orientation from that in Fig. 1(b), i.e., Pd(111) is no longer parallel to CZO (111), but instead tilted about 30 degrees.

The most interesting observation obtained from the cross-sectional TEM images is the strong tendency for ceria-zirconia to migrate onto, or wet, Pd particles subjected to the reducing treatment. To confirm this observation, we examined samples subjected to the extended reducing treatment. As shown in Fig. 3(a), the oxide-wetting phenomenon becomes even more prominent than that shown in Fig. 1(b).

An image at higher magnification clearly reveals the crystal lattice of Pd, the underlying ceria-zirconia, and the wetting material, as shown in Fig. 3(b). A Moiré fringe is formed due to the lattice overlap of Pd and the wetting material. The inset at the upper-right corner is a corresponding Fourier transformation (FT) pattern of the HRTEM image, from which an epitaxial orientation relationship between the Pd particle and the oxide can be identified as Pd(111)

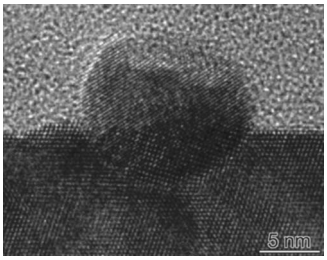

FIG. 2. HRTEM image of a partially encapsulated Pd particle with curved interface.

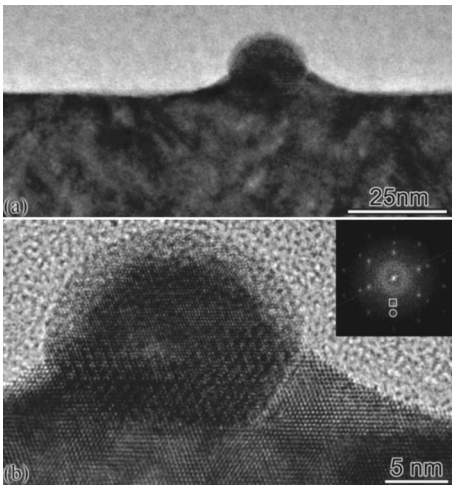

FIG. 3. (a) TEM image of a Pd particle partially encapsulated by wetting material from the CZO support after the extended reduction treatment, (b) HRTEM image of the Pd particle and its interface with the CZO substrate. The inset is the corresponding Fourier transformation pattern, in which the circled spot is from Pd and the squared one is from ceria-zirconia.

$\times$[110]//CZO(111)[110]. No structural difference is found between the wetting material and the oxide film. X-ray energy dispersion spectroscopy (EDS) results shows that the composition of the wetting material is similar to that of the oxide film, although the former may be slightly Ce rich.

As in the case of the metal-titania interaction, in which reduction of Ti^{+4} is required,[4] reduced Ce^{+4} (i.e., Ce^{+3}) is likely to be central to the Pd-ceria interaction. In order to determine the valence of Ce in the ceria-zirconia thin film, we performed an electron energy loss spectroscopy (EELS) study. The identification of the valence of Ce is based on the intensity ratio of its M_4 and M_5 energy loss peaks. For Ce^{+4}, M_4/M_5 is $\sim$1.1, while for Ce^{+3}, the ratio is $\sim$0.78.[19]

Figure 4(a) shows EELS spectra of Ce from the

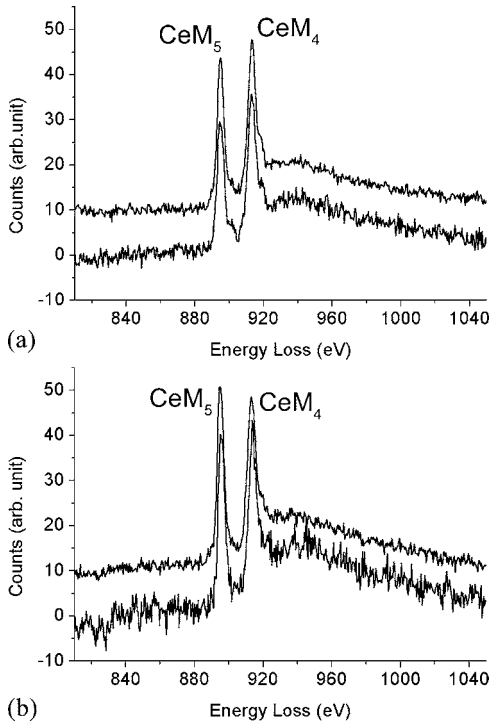

FIG. 4. EELS spectra of Ce from surface (curve 1) and interface (curve 2) regions of the (a) calcined and (b) reduced samples.

$Ce_{0.7}Zr_{0.3}O_2$ thin film for the film surface (curve 1) and film/substrate (YSZ) interface (curve 2) regions of the calcined sample. It is clear that the Ce M4/M5 peak ratio is larger than 1 at both of these regions of the CZO film, which indicates that all Ce ions in the calcined sample are Ce^{+4}. Figure 4(b) shows EELS spectra from the reduced sample. The Ce M_4/M_5 peak ratio of the spectrum from the region near the film/substrate interface remains larger than 1 albeit less than that in Fig. 4(a), while the Ce M_4/M_5 ratio of the spectrum from the film surface is now smaller than 1. These results indicate that Ce ions at the film surface change from Ce^{+4} to Ce^{+3} upon reduction, and the Ce^{+3}/Ce^{+4} ratio is higher near the surface than near the film/YSZ substrate interface. Thus, there is a Ce^{+3} concentration gradient from the interface to the surface for the reduced CZO thin film.

During reduction, lattice-oxygen atoms from the surface of CZO react with H_2 and CO to form H_2O and CO_2 and leave oxygen vacancies (O_v) in the oxide. After reduction, the population of oxygen vacancies near the film surface is high, and according to recent quantum mechanical calculations,[10] the most favorable location of Ce^{+3} is next to oxygen vacancies. In this way, the concentration of Ce^{+3} at the film surface will also be high, which creates a driving force for diffusion of O_v and Ce^{+3} into the CZO film. However, it is difficult for Ce^{+3} to diffuse into the bulk because the ionic radius of Ce^{+3} (0.1283 nm with a coordination number of 8) is larger than that of Ce^{+4} (0.111 nm).[20] In fact, it has been recently shown that surface Ce ions are essentially immobile with respect to diffusion *into* the bulk of a CeO_2 single crystal during high temperature annealing in vacuum.[21] Thus, Ce^{+3} will become enriched at the surface, as revealed by EELS.

One consequence of the Ce^{+3} enrichment is that the increase in average cation radius will expand the lattice parameters and introduce a compressive stress in the top layer of the CZO surface. The thickness of this reduced and stressed layer is determined by the reduction conditions. This stress could, in turn, provide the driving force for diffusion of oxide cations and anions along the *CZO surface* toward Pd particles, where eruption of the support material around the Pd particles, causing their partial encapsulation, would release the stress.

While this process may occur for Pd particles whose close-packed (111) planes are parallel to the CZO (111) surface (observed most often), for the Pd particle that is tilted so that its (111) plane is not parallel to the CZO (111) plane, a different process apparently takes place, as shown in Fig. 2. Although rare, this situation provides an indication of the importance of crystal orientation to the metal-oxide interaction. When the Pd particle is tilted away from the epitaxial orientation, Pd(111)//CZO(111), a metal/oxide interface with relatively higher interfacial energy will be generated due to the larger lattice mismatch. This, in turn, could lead to a high rate of diffusion of oxide cations and anions along the *metal-oxide interface* toward the CZO surface, eventually allowing the particle to sink into the oxide substrate. Apparently, a curved interface is favored in this case.

It is worth mentioning that when YSZ (111) was used as support instead of CZO (111), we did not find any tendency toward Pd particle encapsulation. This confirms that Ce is essential to the SMSI interaction in the Pd/CZO system.

In summary, two distinct processes of partial encapsulation of Pd particles by their reduced CZO support surface have been found: (1) An oxide-wetting behavior that occurs when the Pd particles exhibit their preferred orientation, Pd(111)∥CZO(111). The oxide diffusion in this case may be driven by relaxation of a compressive stress produced by CZO lattice expansion due to the larger ionic radius of Ce^{+3} than Ce^{+4}. (2) A particle-sinking behavior that occurs when the Pd particles are not epitaxially oriented on the CZO surface. In this case, oxide diffusion may more likely be along the high-energy interface between the metal and oxide. In both instances, however, the fundamental principle involved in allowing the system to relax is minimization of total energy. Reducible Ce^{+4} is central to the Pd-CZO interaction. The characteristics of the metal-oxide interaction thus depend on both properties of the oxide (and possibly the metal) as well as their relative crystallographic orientations.

The ceria-zirconia thin-film single crystals used in this study were prepared at the Environmental Molecular Sciences Laboratory, a national scientific user facility sponsored by the U. S. Department of Energy's (DOE) Office of Biological and Environmental Research and located at Pacific Northwest National Laboratory. The TEM work was performed in the Electron Microbeam Analysis Laboratory (EMAL) at the University of Michigan using a JEOL 2010F TEM with NSF award number DMR-9871177. The authors gratefully acknowledge the support from the DOE's Office of Basic Energy Sciences, Division of Chemical Sciences, Ford Motor Company through a University Research Program grant, and National Science Foundation (NSF) through Grant No. NSF/DMR 9875405 (CAREER, XQP).

[1] M. Bäumer and H.-J. Freund, Prog. Surf. Sci. **61**, 127 (1999).
[2] A. Y. Stakheev and L. M. Kustov, Appl. Catal., A **188**, 3 (1999).
[3] D. R. Rainer and D. W. Goodman, J. Mol. Catal. A: Chem. **131**, 259 (1998).
[4] S. J. Tauster, Acc. Chem. Res. **20**, 389 (1987).
[5] R. A. Bennett, P. Stones, and M. Bowker, Catal. Lett. **59**, 99 (1999).
[6] J. M. Gatica, R. T. Baker, P. Fornasiero, S. Bernal, and J. Kašpar, J. Phys. Chem. B **105**, 1191 (2001).
[7] R. T. Baker, S. Bernal, J. J. Calvino, J. M. Gatica, C. López Carts, and J. A. Pérez Omil, Inst. Phys. Conf. Ser. **168**, 417 (2001), Section 9.
[8] S. Bernal, G. Blanco, J. J. Calvino, C. López-Carts, J. A. Pérez Omil, J. M. Gatica, O. Stephan, and C. Colliex, Catal. Lett. **76**, 131 (2001).
[9] R. W. McCabe and J. M. Kisenyi, Chem. Ind. **15**, 605 (1995).
[10] N. V. Skorodumova, S. I. Simak, B. I. Lundqvist, I. A. Abrikosov, and B. Johansson, Phys. Rev. Lett. **89**, 166601 (2002).
[11] H.-W. Jen, G. W. Graham, W. Chun, R. W. McCabe, J.-P. Cuif, S. E. Deutsch, and O. Touret, Catal. Today **50**, 309 (1999).
[12] G. W. Graham, H.-W. Jen, R. W. McCabe, A. M. Straccia, and L. P. Haack, Catal. Lett. **67**, 99 (2000).
[13] G. W. Graham, H.-W. Jen, W. Chun, and R. W. McCabe, J. Catal. **182**, 228 (1999).
[14] G. W. Graham, H.-W. Jen, W. Chun, and R. W. McCabe, Catal. Lett. **44**, 185 (1997).
[15] J. C. Jiang, X. Q. Pan, G. W. Graham, R. W. McCabe, and J. Schwank, Catal. Lett. **53**, 37 (1998).
[16] A. Badri, C. Binet, and J.-C. Lavalley, J. Chem. Soc., Faraday Trans. **92**, 1603 (1996).
[17] B. R. Powell and S. E. Whittington, J. Catal. **81**, 382 (1983).
[18] Y. Gao, G. S. Herman, S. Thevuthasan, C. H. F. Peden, and S. A. Chambers, J. Vac. Sci. Technol. A **17**, 961 (1999).
[19] J. A. Fortner, E. C. Buck, A. J. G. Ellison, and J. K. Bates, Ultramicroscopy **67**, 77 (1997).
[20] M. Barsoum, *Fundamentals of Ceramics* (McGraw-Hill, New York, 1997).
[21] C. L. Perkins, M. A. Henderson, C. H. F. Peden, and G. S. Herman, J. Vac. Sci. Technol. A **19**, 1942 (2001).